Circ-GALNT16 Restrains Colorectal Cancer Progression by Enhancing the SUMOylation of hnRNPK

Chaofan Peng
Nanjing Medical University
Yuqian Tan
Nanjing Medical University
Peng Yang
Nanjing Medical University
Kangpeng Jin
Nanjing Medical University
Chuan Zhang
Nanjing Medical University
Wen Peng
Nanjing Medical University
lu Wang
Nanjing Medical University
Jiahui Zhou
Nanjing Medical University
Ranran Chen
Nanjing Medical University
Tuo Wang
Nanjing Medical University
Chi Jin
Nanjing Medical University
Jiangzhou Ji
Nanjing Medical University
Yifei Feng
Nanjing Medical University
Junwei Tang
Nanjing Medical University
Yueming Sun (sunyueming@njmu.edu.cn)
Nanjing Medical University

Research Article

Keywords: Colorectal cancer, circ-GALNT16, hnRNPK, SUMOylation, p53, Serpine1, SENP2

Posted Date: May 17th, 2021

DOI: https://doi.org/10.21203/rs.3.rs-501100/v1

Abstract

Background

Emerging studies have investigated circRNAs as significant regulation factors in multiple cancer progression. Nevertheless, the biological functions and underlying mechanisms of circRNAs in colorectal cancer progression remain unclear.

Methods

A novel circRNA (circ-GALNT16) was identified by microarray and qRT-PCR. A series of phenotype experiments *in vitro* and *vivo* were performed to investigate the role of circ-GALNT16 in CRC. FISH, RNA pulldown assay, RIP assay, RNA sequencing, coimmunoprecipitation, and ChIP were constructed to explore the molecular mechanisms of circ-GALNT16 in colorectal cancer.

Results

Circ-GALNT16 was downregulated in colorectal cancer and negatively correlated with poor prognosis. Circ-GALNT16 suppressed the proliferation and metastasis ability of colorectal cancer *in vitro* and *vivo*. Mechanistically, circ-GALNT16 could bind to the KH3 domain of heterogeneous nuclear ribonucleoprotein K (hnRNPK), which resulted in the SUMOylation of hnRNPK. Additionally, circ-GALNT16 could enhance the hnRNPK-p53 complex by facilitating the SUMOylation of hnRNPK. Furthermore, RNA sequencing assay identified serpin family E member 1 as the target gene of circ-GALNT16 at the transcriptional level. Rescue assays revealed that circ-GALNT16 regulated the expression of Serpine1 by inhibiting the deSUMOylation of hnRNPK mediated by SUMO specific peptidase 2 and then regulating the sequence-specific DNA binding ability of the hnRNPK-p53 transcriptional complex.

Conclusions

Circ-GALNT16 suppressed CRC progression via inhibiting Serpine1 expression through adjusting the sequence-specific DNA binding ability of the SENP2-mediated hnRNPK-p53 transcriptional complex and might work as a biomarker and therapeutic target for CRC.

Background

Colorectal cancer (CRC) is one of the most common malignant tumors and continues to be a serve health problem (1). The incidence and mortality rank third and second, respectively, among cancers according to the up-to-date global cancer statistics. The prognosis of advanced patients remains poor, although neoadjuvant chemoradiotherapy, surgery, post-operative chemoradiotherapy, and immunotherapy are widely performed and developing rapidly (2). One of the leading causes is that the detailed mechanisms of CRC progression remain unclear. So, it's urgent to explore the unknown pathogenic mechanisms of CRC to develop specific diagnostic makers and accurate therapeutic targets.

Circular RNA (circRNA) is a kind of transcripts characterized by originating from the back-splicing of pre-mRNA (3, 4). CircRNAs have higher stability than liner transcripts and are more resistant to RNase R due to their loop structure, which makes circRNAs potential diagnostic markers and therapeutic targets for cancer (5, 6). The biological functions of circRNAs are widely involved in the proliferation, metastasis, apoptosis, and autophagy of various cancers via multiple ways (7–10). For example, hsa_circ_101555 can promote colorectal cancer progression through acting as a competing endogenous RNA of miR-597-5p (11). Circ-ABCC1 binds to β-catenin and activates the Wnt/β-catenin pathway to facilitate CRC progression (12). CircPPP1R12A can encode a novel protein to promote colon cancer pathogenesis through Hippo-YAP signaling (13). However, the detailed mechanisms of how circRNAs regulate the CRC progression remain elusive.

To explore the role of circRNA in CRC proliferation and metastasis, a circRNA microarray was constructed to detect circRNAs in human CRC and adjacent tissues and identified a novel circRNA named circ-GALNT16 (circBase ID: has_circ_0102495), which is generated from the back-splicing of GALNT16 mRNA (exon1) on chromosome 14 and has 290 nucleotides in length. Circ-GALNT16 was extremely down-regulated in CRC tissues, and low circ-GALNT16 expression correlated with poor prognosis, while its function in CRC progression remained unclear. In addition, circ-GALNT16 knockdown promoted the proliferation and metastasis of CRC *in vivo* and *vitro*, while circ-GALNT16 overexpression had converse effects. These results showed that circ-GALNT16 might serve as a potential diagnostic biomarker and therapeutic target for CRC.

HnRNPK is a DNA and RNA binding protein, which regulates extensive biological processes, including transcriptional regulation, nucleocytoplasmic transport, and DNA damage repair (14). In cancer, some studies have identified hnRNPK as an oncogene due to its overexpression in several cancer tissues, while hnRNPK has also been identified as an antioncogene because of its activation of p53 pathway. SUMOylation is a kind of posttranslational modification of hnRNPK by conjugating a small ubiquitin-like modifier (SUMO) covalently via a multi-step reaction (15). The SUMOylation of hnRNPK may regulate RNA metabolism at the transcriptional and post-transcriptional levels (16). Several studies have reported that the SUMOylation of hnRNPK could enhance the interaction between hnRNPK and p53 and regulate the transcriptional activity of p53 (17–19).

In this study, we elucidated that circ-GALNT16 could suppress CRC progression by enhancing the SUMOylation of hnRNPK to regulate the sequence-specific DNA binding ability of the hnRNPK-p53 complex. Collectively, our study investigated that circ-GALNT16 mediated specific molecular mechanisms in CRC progression, which might contribute to exploring a potential diagnostic marker and therapeutic target for CRC.

Methods

Microarray analysis of CircRNAs

The circRNA microarray analysis (CapitalBio Technology, Beijing, China) consisted of specifical probes targeting back-splicing sites of human circRNAs was performed. The circRNAs in 5 pairs of CRC tissues were detected. The data normalization, summarization, and quality control were analyzed by the GeneSpring software. The differential circRNAs are listed in Table S1. All the raw data of the microarray analysis can be found in the Gene Expression Omnibus with the number GSE172229.

Patient samples and cell culture

One hundred CRC patients' tumor samples and paired adjacent normal tissues were collected between 2014 and 2018 from the department of general surgery, First Affiliated Hospital of Nanjing Medical University. Fresh tissues were acquired after surgery and immediately frozen at -80°C. Patients who had received neoadjuvant chemoradiotherapy were excluded. This study was approved by the Human Ethics Committee of First Affiliated Hospital of Nanjing Medical University. Each patient was informed about the study and consented to the specimen donation before the surgery. The raw data of circ-GALNT16 expression in 100 pairs of CRC tissues and relative expression in different pathological subgroups are listed in Table S2.

LoVo, DLD-1, SW-480, Caco-2, RKO, HCT 116, HT-29, NCM460 were purchased from Cell Bank of Type Culture Collection of the Chinese Academy of Science (Shanghai, China) and cultured under recommended medium with 10% fetal bovine serum at 37°C in a 5% CO2 humidified incubator.

RNA extraction and qRT-PCR

Total RNA was extracted from patients’ specimens and cells by TRIzol reagent (Invitrogen, USA), and the procedures were applied as previously described (20). Then, a PrimeScript RT reagent kit (TaKara, Dalian, China) was used for reverse transcription. An SYBR Premix Ex Taq Kit (TaKara) was used for the qRT-PCR experiment on Applied Biosystems 7500 sequence Detection System. GAPDH was used as an internal control. The primers’ sequences are listed in Table S3.

Cell Transfection

The lentivirus containing shRNAs and full-length targeting circ-GALNT16, including corresponding negative control, were synthesized by Obio (Shanghai, China). Serpine1 overexpression plasmid was obtained from Obio. Obio synthesized the truncated hnRNPK plasmids of hnRNPK with a C-terminus 3× Flag tag. The small interfering RNA (siRNA) oligonucleotides targeting hnRNPK, SENP2, and Serpine1 were synthesized by RiboBio (Guangzhou, China). Procedures were described previously, using Lipofectamine 3000 (Invitrogen) (21). The shRNAs and siRNAs sequences are listed in Table S3.

Cell proliferation assays

Cell proliferation assays, including Cell Counting Kit-8 and colony formation assay, were performed as described previously (22). The cell proliferation ability was measured via the 5-Ethynyl-2'-deoxyuridine assay using an EdU kit (Beyotime, Shanghai, China).

Transwell and scratch wound healing assay

Transwell assay was performed with Millipore cell culture inserts (24-well insert, 8-μm pore size). 3×10^4 cells resuspended in 200μL serum-free medium per well were seeded into the upper chamber of Transwell membrane while the lower layer was filled with 700μL culture medium containing 10% serum for migration assay. After 24h (36 or 48h based on different cell lines), we stained the cells on the underside of the membrane using crystal violet solution and wiped out the cells above the membrane with swabs. Five random views were counted in each well under a microscope. For invasion assay, Matrigel (BD Biosciences, Franklin Lakes, NJ, USA) was spread on the upper layer, and the rest of procedures were followed the steps described above.

A 200μL pipette tip was used to produce consistent length lesions in six-well plates (8×10^5 cells per well) for wound healing assay. An inversion microscope was used to take each wound image at 0 and 48 h. We used ImageJ to quantitatively evaluate the gap distance.

Flow cytometry assay of cell cycle and apoptosis

Treated cells were fixed in 75% alcohol overnight at -20°C for cell cycle assay. The cells were washed three times, and a Cell Cycle Analysis Kit (Beyotime, Shanghai, China) was used for propidium iodide (PI) staining.

For apoptosis analysis, all cells were treated with 0.5 mM of H_2O_2 for 4 h to stimulate apoptosis. An Annexin VAPC/7-AAD Apoptosis Detection Kit (KeyGEN, Jiangsu, China) was used for Annexin V-APC and 7-AAD staining according to the protocol. Finally, the percentage of cell cycle distribution and apoptotic rate were analyzed using BD FACSCanto II (BD Biosciences, San Jose, CA, USA).

Animal models

Four weeks old male BALB/c nude mice were purchased from the Animal Center of Nanjing Medical University (Nanjing, China) for subcutaneous tumor formation and liver metastasis model. For the xenograft model, 10^6 DLD-1 cells transfected with sh-circ-GALNT16#1 and RKO cells transfected with circ-GALNT16, as well as corresponding control cells, were resuspended in 1mL PBS (phosphate-buffered saline), and respectively subcutaneous injected into the left and right armpits of the mice. Each tumor volume was calculated every five days since the tumor became macroscopic. All the mice were sacrificed 30 days after the subcutaneous injection, and the xenograft tumors were weighed and obtained for IHC.

10^6 cells suspended in 20μL PBS were injected into the distal tip of the mice's spleen to establish the metastatic model. The liver tissues were dissected and embedded in paraffin for H&E staining 6 weeks later. All these animal experiments were ratified by the Committee on the Ethics of Animal Experiments of Nanjing Medical University.

Immunohistochemistry

Immunohistochemistry (IHC) was performed as previously described (22). All the antibodies used are listed in Table S4.

RNA and protein isolation of nuclear and cytoplasmic fractions

Nuclear and cytoplasmic fractions of CRC cells were separately isolated with a PARIS™ kit (AM1556, Thermo Fisher Scientific, Waltham, USA). RNA was isolated according to the protocol and analyzed through qRT-PCR. U6, 18S, and GAPDH were used as internal controls. The isolated nuclear protein was prepared for subsequent pulldown assay.

Fluorescence in situ hybridization and Immunofluorescence

Circ-GALNT16 specifical Cy3-labelled probe was applied to detect the subcellular localization of circ-GALNT16 in DLD-1 and LoVo using a FISH Kit (RiboBio). Briefly, after cells were fixed with paraformaldehyde for 10min and permeabilized for 5min using PBS with 0.5% Triton X-100, FISH probe hybridized with preheated hybridization buffer was mixed with cells at 37°C overnight. Then, the cells were washed with 4×sodium citrate buffer containing 0.1% Tween-20 for 5 min and 1× SSC for 5 min. The cell nucleus was stained with 4,6-diamidino-2-phenylindole (DAPI). The images were obtained using a confocal fluorescence microscope.

For dual RNA-FISH and immunofluorescence assay, an immunostaining blocking solution (Beyotime) was used for cell blocking for 1 h after incubated with the FISH probe as described above. Then cells were incubated with hnRNPK antibody overnight and labeled with fluorescent secondary antibody for 1h under dark condition. Finally, DAPI was used for nuclear staining.

RNA pulldown assay and mass spectrometry

Biotin labeling pulldown probe targeting circ-GALNT16 and control probe were designed and synthesized by Ribobio. RNA pulldown assay was constructed using Pierce Magnetic RNA-Protein Pull-Down Kit according to the protocol (#20164, Thermo). Mass spectrometry analysis was performed in the elution protein extracted from RNA pulldown assay. The differential proteins identified by mass spectrometry and the RNA binding proteins list (RBPs; http://www.ablife.cc) are shown in Table S5.

Western blot

Western blot (WB) was carried out as previously reported (20). The antibodies are shown in Table S4.

RIP and Coimmunoprecipitation assay

RNA immunoprecipitation (RIP) assay was performed using a RIP Kit (Millipore, Burlington, MA, USA). In Brief, 5μg anti-hnRNPK or anti-FLAG antibody and magnetic beads were mixed and incubated with cells lysis lysed by RIP lysis buffer supplemented with protease and RNase inhibitors overnight at 4°C. The immunoprecipitated RNA was obtained for qRT-PCR after being digested with proteinase K buffer.

Coimmunoprecipitation assay was constructed with an IP/Co-IP Kit (#88828, Thermo) to explore the interactions between hnRNPK with p53 and SENP2. The detailed procedures were performed as

previously described (23).

SUMOylation modification analysis

The treated cell lysate was diluted 20-fold with lysis buffer consisted of 20mM Tris-HCl (PH = 8.0), 150mM NaCl, 2 mM NEM, 1 × protease inhibitor cocktail, and 0.2% Triton X-100. The lysate was incubated with anti-hnRNPK for 4 hours at 4°C. Then, the lysate was mixed and incubated with protein A/G-Sepharose (sc-2003; Santa Cruz, USA) overnight at 4°C. Resins were washed with lysis buffer with 1% Triton X-100 for three times and boiled in 50μL SDS sample buffer for 10 min. Finally, WB was performed with supernatants using anti-hnRNPK and anti-SUMO1.

RNA sequencing assay

RNA-seq libraries were prepared after RNA-seq was constructed in RKO cells transfected with circ-GALNT16 overexpression lentivirus and control cells. Firstly, RNA samples that had passed quality inspection were constructed with a starting amount of 1μg and performed RNA Integrity checking by Agilent 4200 TapeStation. The key steps were as follows: RNA purification by polyA Oligo magnetic beads; first-strand cDNA synthesis with random hexamer primers; RNA degradation with RNase H and second-strand cDNA synthesis using DNA polymerase I; double-stranded cDNA fragments end repair and the addition of a single 'A' base at the 3'-end of each strand; special sequencing adapters ligation; PCR amplification. Finally, a HiSeq 2000 system on Pair End (Illumina, San Diego, CA, USA) was used to sequence the purified cDNA. The mRNA sequencing results are shown in Table S6.

Chromatin immunoprecipitation assays

A ChIP Kit (CST, #56383, Danvers, MA, USA) was used for ChIP assays following the protocol. Briefly, chromatin fragments were sheared to be concentrated on 200 to 1000 bp through ChIP sonication lysis buffers. Then beads-antibody complexes were incubated with sheared crosslinked chromatin. After the DNA was purified, qRT-PCR was performed using ChIP primers. The sequences of ChIP primer are listed in Table S3.

Statistical analysis

Each experiment was repeated at least three times. All the statistical analyses were carried out with GraphPad Prism software (La Jolla, CA, USA) and SPSS 13.0 software (Chicago, IL, USA). Student's t-test was performed to analyze the difference between two samples, while ANOVA was used for tests among more than two groups. Pearson correlation analysis was performed to estimate the correlation between circ-GALNT16 and Serpine1. Chi-square test was used to analyze the correlation between circ-GALNT16 expression in tumor tissues and relative clinicopathologic data. Overall survival (OS) rates were estimated using Kaplan-Meier analyses. The significance threshold of each test was set at 0.05.

Results

Circ-GALNT16 is downregulated in CRC tissues and correlates with good prognosis

To explore pivotal circRNAs involved in CRC progression, a circRNA microarray was constructed in matched CRC and adjacent normal tissues from 5 patients, and the top 20 upregulated and downregulated circRNAs were shown by heatmap (Fig. 1a). We selected the top ten differential expression circRNAs (P value < 0.01) for further tumor tissues qRT-PCR verification in 20 paired tumor tissues (Fig. S1a). Circ-GALNT16 (circBase ID: hsa_circ_0102495) had an extreme downregulation in CRC tissues among them. Therefore circ-GALNT16 was chosen for our in-depth study. Circ-GALNT16 is generated from the exon1 of GALNT16 gene located on chromosome 14 and has 290 nucleotides in length according to the circBase annotation. Sanger sequencing was performed to validate the back-splicing of circ-GALNT16 (Fig. 1b). To confirm the circular formation of circ-GALNT16, both convergent and divergent primers were designed to amplify the linear and back-splicing products. The results demonstrated that the convergent primers for both circ-GALNT16 and GAPDH could amplify products of expected size from both complementary DNA (cDNA) and genomic DNA (gDNA). While only divergent primers for circ-GALNT16, but not GAPDH, could amplify a PCR product from cDNA, but not gDNA (Fig. 1c and Fig. S2a). In addition, qRT-PCR confirmed that circ-GALNT16 was more resistant to RNase R and actinomycin D treatment than GALNT16 mRNA in DLD-1 and LoVo (Fig. 1d, e and Fig. S2b, c). These results indicated that circ-GALNT16 is a circular, not linear structure. Circ-GALNT16 was remarkably downregulated in 100 CRC tissues compared with paired adjacent normal tissues (Fig. 1f and Fig. S2d). Correspondingly, the expression of circ-GALNT16 in normal colorectal epithelial cells NCM460 was significantly higher than in CRC cell lines (Fig. S2e). The correlation between circ-GALNT16 expression level and clinical subgroups was analyzed. The expression of circ-GALNT16 was negatively correlated with tumor size, tumor stage, and lymphatic node metastasis (Fig. 1g, h and Fig. S2f). To further investigate the connection between circ-GALNT16 expression level and clinical characteristics, the specimens were separated into two groups according to the median of circ-GALNT16 expression. As shown in Table 1, there were significant differences in tumor size, stage, and lymphatic node metastasis but no difference in gender, age, and carcinoembryonic antigen (CEA) level between high and low circ-GALNT16 expression groups. In addition, lower circ-GALNT16 expression in tumor tissues was correlated with shorter overall survival (Fig. 1i). All these clinical data suggested that circ-GALNT16 is downregulated in CRC and may work as a potential diagnostic and prognostic biomarker for CRC.

Table 1
Relevance analysis of circ-GALNT16 expression in CRC patients(n = 100).

Table.1 Relevance analysis of circ-GALNT16 expression in CRC patients.				
Variables	**All patients**	**circ-GALNT16**		**P-value**
		Low	**High**	
All Cases	100	50	50	
Age (years)				
< 60	35	16	19	0.53
≥ 60	65	34	31	
Gender				
Female	41	18	23	0.31
Male	59	32	27	
Tumor size (cm)				
< 5	55	19	36	**0.001**
≥ 5	45	31	14	
Tumor stage				
Stage I + II	59	22	37	**0.002**
Stage III + IV	41	28	13	
Lymph node metastasis				
No	61	23	38	**0.002**
Yes	39	27	12	
Liver metastasis				
No	93	47	46	> 0.99
Yes	7	3	4	
CEA (ng/ml)				
< 4.70	46	25	21	0.42
≥ 4.70	54	25	29	
NOTE: CEA: carcinoembryonic antigen				
All data are presented as the means ± SD of three independent experiments. P ≤ 0.05 was considered significant. The bold type represents P values smaller than 0.05				

Circ-GALNT16 inhibits the proliferation and metastasis of CRC cells in vitro **and** vivo

Due to the comparatively high expression of circ-GALNT16 in LoVo and DLD-1 cells, three shRNAs against circ-GALNT16 were transfected into LoVo and DLD-1. Meanwhile, a circ-GALNT16 overexpression lentivirus was transfected into RKO and HCT 116 because of their relatively low expression of circ-GALNT16 to explore the roles of circ-GALNT16 in CRC proliferation and metastasis. Knockdown and overexpression efficiency was confirmed by qRT-PCR (Fig. S3a, b). Both sh-circ-GALNT16#1 and sh-circ-GALNT16#2 were chosen for the following cell phenotype assays. CCK-8, colony formation, and EdU assays demonstrated that circ-GALNT16 silencing excessively promoted cell proliferation in LoVo and DLD-1, while overexpression circ-GALNT16 caused a completely contrary phenomenon in RKO and HCT 116 (Fig. 2a-f). Furthermore, flow cytometric assay of cell cycle distribution demonstrated that the knockdown of circ-GALNT16 facilitated the G1 to S transition. However, the overexpression of circ-GALNT16 dramatically increased the rate of G0/G1 phase, along with a striking decrease of S phase cells (Fig. 2g, h). Apoptosis test showed that the CRC cells which were transfected with shRNAs had lower apoptotic rates than the control group. Conversely, the apoptotic rates remarkably increased while circ-GALNT16 was overexpressed in RKO and HCT 116 (Fig. 2i, j). Additionally, transwell and scratch wound healing assays confirmed that circ-GALNT16 depletion prominently enhanced the migration and invasion ability of CRC cells, while overexpression circ-GALNT16 impaired this ability (Fig. 3a-d).

DLD-1 cells, which were stably transfected with sh-circ-GALNT16#1, and RKO cells stably transfected with circ-GALNT16, along with their relative control group, were subcutaneously injected into nude mice to explore the regulation effect of circ-GALNT16 on CRC cells proliferation *in vivo*. The results showed that tumors generated from circ-GALNT16 overexpression cells had less tumor volume and weight than the control group, while circ-GALNT16 depletion had a contrary effect (Fig. 3e and Fig. S3c). Furthermore, Ki-67, C-myc, and Serpine1 expression levels were increased in circ-GALNT16 knockdown group and decreased in circ-GALNT16 overexpression group measured by IHC (Fig. S3d). Tumor metastasis assay confirmed that the depletion of circ-GALNT16 resulted in more liver metastasis nodules. By contrast, circ-GALNT16 overexpression caused less liver metastasis than the control group (Fig. 3f, g). Collectively, all these results illustrate that circ-GALNT16 inhibits the proliferation and metastasis of colorectal cancer *in vitro* and *vivo*.

Circ-GALNT16 suppresses the progression of CRC by specifically binding to the KH3 domain of hnRNPK

To explore the detailed tumor suppression mechanisms of circ-GALNT16 in CRC, we firstly examined the subcellular location of circ-GALNT16 in CRC cells. Subcellular fractionation assay and Fluorescent in sit hybridization (FISH) assay showed that circ-GALNT16 was predominantly located in the nucleus of CRC cells (Fig. 4a, b and Fig. S3e). Next, we performed the biotin-labeled RNA pulldown by circ-GALNT16 specifical probe and control probe in DLD-1 and LoVo, followed by silver staining to identify circ-GALNT16 potential protein partner (Fig. 4c). Mass spectrometry revealed that circ-GALNT16 probe group contained 156 and 96 differential proteins in DLD-1 and LoVo, respectively. After overlapping with RNA

binding proteins, two candidates were selected out for protein partner of circ-GALNT16: heterogeneous nuclear ribonucleoprotein K (hnRNPK) and FKBP prolyl isomerase 4 (FKBP4). Considering the nuclear location of circ-GALNT16, we chose hnRNPK for the potential partner of circ-GALNT16, and western blot verified the results of mass spectrometry (Fig. 4d and Fig. S4a). HnRNPK was reported to work as a DNA and RNA binding protein and regulate a large number of biological processes and cancer pathogenesis (14). Additionally, previous studies had explored that hnRNPK could influence CRC progression by interacting with noncoding RNA (24, 25). Then, hnRNPK silencing cells were constructed (Fig. S4b). RNA pulldown assay was then performed again in nucleoprotein of DLD-1 cells (Fig. S4c). Additionally, RIP assay showed that hnRNPK could specifically enrich circ-GALNT16 (Fig. 4e). Dual RNA-FISH and immunofluorescence assay showed the colocalization of circ-GALNT16 and hnRNPK (Fig. 4f). We designed four truncated hnRNPK plasmids aiming at three K homology (KH) domains that mediate nucleic acid binding to explore which domain circ-GALNT16 interacted with. Protein domain mapping and RIP assay showed that circ-GALNT16 interacted with the KH3 domain of hnRNPK (Fig. 4g-i). Furthermore, CCK8 and transwell assays indicated that circ-GALNT16 depletion could not affect proliferation and metastasis ability of CRC cells while hnRNPK was knockdown (Fig. S4d, e). The mRNA and protein levels of hnRNPK did not alter in circ-GALNT16 knockdown or overexpression cells (Fig. 4j and Fig. S4f). Besides, the expression of circ-GALNT16 remained unchangeable while hnRNPK was knockdown (Fig. 4k). Collectively, circ-GALNT16 restrains CRC progression by interacting with the KH3 domain of hnRNPK.

Circ-GALNT16 enhances hnRNPK-p53 interaction through inhibiting SENP2-mediated hnRNPK deSUMOylation and hnRNPK facilitates the nuclear accumulation of circ-GALNT16

Given that circ-GALNT16 could specifically interact with hnRNPK, we next explored how circ-GALNT16 restrained CRC progression via hnRNPK. Because the protein levels of hnRNPK were not changed in circ-GALNT16 knockdown or overexpression cells, we supposed that circ-GALNT16 could influence some kind of posttranslational modification of hnRNPK through binding to it. Previous studies had reported that the site of hnRNPK SUMOylation is in the KH3 domain, and noncoding RNA could regulate the SUMOylation of hnRNPK in hepatocellular carcinoma. SUMOylation is a vital posttranslational modification of hnRNPK involved in transcriptional regulation, DNA repair, and so on (15, 26). So, we wondered whether circ-GALNT16 could regulate the SUMOylation modification of hnRNPK. Then coimmunoprecipitation assay was performed in protein lysate pulled down by circ-GALNT16 specifical probe, and the results indicated that circ-GALNT16 might mediate the interaction between hnRNPK and SUMO1 (Fig. 5a). Furthermore, SUMOylation modification analysis was performed. The results showed that knockdown of circ-GALNT16 could decrease the SUMOylation modification of hnRNPK in 100kDa, which was the theoretical molecular weight of hnRNPK conjugated with SUMO1 (Fig. 5b). It had been reported that SUMO specific peptidase 2 (SENP2) could antagonistically regulate hnRNPK SUMOylation in HeLa and HCC cells. However, it was still unclear whether SENP2 could facilitate the deSUMOylation of hnRNPK in CRC (17, 26). Co-IP assay confirmed that SENP2 could specially bind to hnRNPK in CRC (Fig. S5a). Then we found that circ-GALNT16 overexpression could impair the interaction between SENP2 and hnRNPK, and circ-GALNT16 knockdown enhanced the interaction (Fig. 5c). Furthermore, SUMOylation modification analysis

elucidated that circ-GALNT16 enhanced the SUMOylation of hnRNPK through SENP2 (Fig. 5d). These data indicated that circ-GALNT16 could weaken the deSUMOylation modification of hnRNPK through binding to hnRNPK and block the interaction between hnRNPK and SENP2.

Plenty of studies had reported that the SUMOylation of hnRNPK could enhance the interaction between hnRNPK and p53, which had an enormous function in cancer progression (17, 18, 26). Co-IP assay indicated that circ-GALNT16 could enhance the interaction between hnRNPK and p53 (Fig. 5e). A previous review summarized three approaches of circRNA in regulating two proteins interactions: regulating the function of one protein but not binding to the other protein; a scaffold cementing their interaction by binding to both of them; acting as a dissociator between two proteins (Fig. 5f) (27). Because circ-GALNT16 did not physically bind to p53, we hypothesized that circ-GALNT16 regulated the interaction between hnRNPK and p53 through enhancing the SUMOylation of hnRNPK, rather than acting as a scaffold between hnRNPK and p53(Fig. 5g and Fig. S5b). Furthermore, SENP2 silencing could abolish the dissociation between hnRNPK and p53 and the proliferation promotion effect of CRC cells caused by the knockdown of circ-GALNT16 (Fig. 5h, Fig. S5c, d). Collectively, circ-GALNT16 can enhance the interaction between hnRNPK and p53 through blocking SENP2-mediated deSUMOylation of hnRNPK.

Meanwhile, after we proved that circ-GALNT16 could specifically interact with hnRNPK and hnRNPK was reported to play a pivotal role in RNA transcription and alternative splicing, we wondered whether hnRNPK could regulate the transcription or splicing of circ-GALNT16 (28–30). Nevertheless, neither circ-GALNT16 nor GALNT16 showed significant variation while hnRNPK was knockdown, indicating that hnRNPK did not participate in the transcription or splicing of circ-GALNT16 (Fig. S6a). A previous study reported that hnRNPK played an extreme role in driving long noncoding RNA nuclear enrichment(31). Considering that most circular RNAs mainly localize in cytoplasm and function as miRNA sponge, but circ-GALNT16 had a nuclear localization, we performed RNA FISH and subcellular fractionation assay again in hnRNPK-depletion cells, which showed that circ-GALNT16 tended to accumulate in the cytoplasm of low hnRNPK expression cells (Fig. S6b, c). These results indicated hnRNPK might contribute to the nuclear localization of circ-GALNT16.

Circ-GALNT16 suppresses CRC proliferation and metastasis through downregulating Serpine1

Given that circ-GALNT16 could enhance the level of the hnRNPK-p53 transcriptional complex, RNA-seq was performed in circ-GALNT16 overexpression and related control RKO cells to find out how circ-GALNT16 regulated CRC progression in transcriptional level (Fig. 6a). 265 genes were downregulated, and 221 genes were upregulated (Fig. 6b). The expression analysis of the top 30 differential genes in CRC tissues was performed according to the public GEPIA dataset based on the TCGA (http://gepia.cancer-pku.cn/index.html). Nine genes were selected for target candidates of circ-GALNT16. Furthermore, the qRT-PCR results showed that only Serpine1 could be downregulated by circ-GALNT16 overexpression but show no significant difference while hnRNPK was silenced (Fig. 6c). Coincidentally, published reports and the KEGG (Kyoto Encyclopedia of Genes and Genomes) pathway database indicated that Serpine1 could

be regulated by p53 (32). Then mRNA and protein level of Serpine1 in circ-GALNT16 knockdown and overexpression cells elucidated that Serpine1 could be antagonistically regulated by circ-GALNT16 (Fig. 6d, e). The expression of Serpine1 in 52 tumor tissues was detected, and the results showed that Serpine1 mRNA level was negatively correlated with circ-GALNT16 expression (Fig. 6f). Then we analyzed the correlation between Serpine1 expression and relative clinical features from TCGA. Serpine1 was upregulated in CRC tissues and positively correlated with advanced tumor stage, lymphoid metastasis, and lower overall survival rate (Fig. 6g-j). These features were contrary to the characteristics of circ-GALNT16, so we hypothesized that circ-GALNT16 might suppress CRC progression by inhibiting Serpine1 expression. Firstly, Serpine1 specifical siRNA was transfected into DLD-1 and LoVo, and overexpression plasmid was transfected into RKO and HCT 116 (Fig. S7a). Phenotype assays illustrated that Serpine1 silencing could remarkably decrease the proliferation and metastasis ability in circ-GALNT16 knockdown cells. On the contrary, Serpine1 overexpression could promote the proliferation and metastasis ability of circ-GALNT16 overexpression cells (Fig. S7b-g and Fig. S8a-d). Taken together, these results show that circ-GALNT16 suppresses CRC through downregulated Serpine1.

Circ-GALNT16 attenuates Serpine1 and enhances p21 mRNA expression level through regulating the sequence-specific DNA binding ability of the hnRNPK-p53 complex

Given that circ-GALNT16 could enhance the hnRNPK-p53 complex and Serpine1 was a p53 target gene, we hypothesized that circ-GALNT16 might regulate Serpine1 by enhancing the level of the hnRNPK-p53 complex. Firstly, we observed that the inhibition effect on Serpine1 caused by circ-GALNT16 could be abolished by hnRNPK silencing (Fig. 7a, b). Meanwhile, considering the previous study reported that SUMOylation of hnRNPK could regulate the sequence-specific DNA binding ability of p53 and exert different adjusting effects on individual p53 target gene, the expression of p21, a representative p53 target antioncogene, was detected together with Serpine1. P21 was downregulated by circ-GALNT16 knockdown and upregulated by circ-GALNT16 overexpression but showed no striking divergence while hnRNPK was knockdown at the same time (Fig. S9a, b). Additionally, the expression of Serpine1 showed no significant difference in circ-GALNT16 depletion cells while SENP2 was silenced, indicating that the SUMOylation of hnRNPK played a vital role in Serpine1 regulation caused by circ-GALNT16 (Fig. 7c). The inhibition effect of circ-GALNT16 knockdown on p21 mRNA level was abolished by SENP2 silencing (Fig. S9c). Furthermore, Pifithrin-α, a specific inhibitor of p53 transcriptional activity, could rescue the Serpine1 expression promotion effect caused by circ-GALNT16 knockdown (Fig. 7d). Pifithrin-α could also abolish the promotion effect of circ-GALNT16 overexpression on p21 mRNA level (Fig. S9d). Chromatin immunoprecipitation assays revealed that circ-GALNT16 depletion enhanced the binding of hnRNPK and p53 to the promoter region of Serpine1 and decreased the binding to the promoter region of p21, which were consistent with the prior results. Circ-GALNT16 overexpression had a contrary effect (Fig. 7e, f and Fig. S9e, f). All these results elucidate that circ-GALNT16 regulates Serpine1 and p21 expression by adjusting the sequence-specific DNA binding ability of the SENP2-mediated hnRNPK-p53 complex.

Circ-GALNT16 regulates CRC progression via PI3K/AKT pathway

Because several studies had reported that Serpine1 could regulate PI3K/AKT pathway, the AKT and p-AKT expression levels, as well as the key protein of cell cycle and apoptosis, were detected (33–35). Circ-GALNT16 knockdown increased the protein levels of Serpine1, p-AKT, Cyclin D1, CDK4, Bcl-2 and negatively regulated Bax level. Conversely, circ-GALNT16 overexpression resulted in opposite results. HnRNPK, p53, and AKT remained unchanged. In addition, Serpine1 silencing rescued the regulation effects in sh-circ-GALNT16 cells. Opposite effects were shown in Serpine1 overexpression and circ-GALNT16 overexpression co-transfected cells (Fig. 8a, b).

Discussion

Several studies indicate that circRNAs, a group of novel noncoding RNAs, can regulate cancer progression via multiple approaches such as serving as miRNA sponges, interacting with proteins, and have the potential to work as critical clinical diagnostic and prognostic biomarkers for malignant tumors (36–39). In this study, we explored a novel circRNA, circ-GALNT16, as a tumor suppressor in CRC. Circ-GALNT16 was found downregulated in CRC tissues and cells. The lower expression of circ-GALNT16 predicated advanced tumor size, tumor stage, lymphatic metastasis, and poor prognosis. Our phenotype experiment and mice model revealed that circ-GALNT16 suppressed the proliferation, migration, and invasion ability of CRC cell lines. Significantly, circ-GALNT16 enhanced hnRNPK-p53 interaction by inhibiting the SENP2-mediated deSUMOylation of hnRNPK, which regulated the sequence-specific DNA binding ability of the hnRNPK-p53 complex (Fig. 8c).

Recent studies covering the functions of circRNAs focused on serving as competing endogenous RNAs (ceRNAs) of miRNAs in the cytoplasm (40, 41). Nevertheless, we accidentally found that circ-GALNT16 predominately located in the nucleus of CRC cells, excluding the possibility of being a miRNA sponge. The mechanisms of circRNAs with nuclear localization in tumor progression remain obscure and poorly investigated, especially in CRC. In the current study, we found that circ-GALNT16 could bind to the KH3 domain of hnRNPK specifically, which is a multifunctional protein involved in transcriptional regulation, RNA splicing, RNA translocation, and chromatin remodeling (14, 28, 31). Furthermore, we found that circ-GALNT16 could enhance the interaction between hnRNPK and p53 via inhibiting SENP2-mediated deSUMOylation of hnRNPK. Then RNA-seq and qRT-PCR validation indicated that circ-GALNT16 could downregulate oncogene Serpine1 and upregulated antioncogene p21 through regulating the sequence-specific DNA binding ability of the hnRNPK-p53 transcriptional complex. Collectively, our study illustrated that circ-GALNT16/hnRNPK/p53 axis could suppress Serpine1 and PI3K/AKT signal pathway in CRC.

Plenty of studies have demonstrated that various posttranslational modifications of hnRNPK, including phosphorylation, ubiquitination, methylation, and SUMOylation, play critical roles in hnRNPK function coactivation (15). Although several circRNAs have been reported to interact with hnRNPK, the circRNA that regulates the posttranslational modification of hnRNPK has not been reported yet (24, 25, 42). On top

of that, the role of circRNA in the SUMOylation of protein has not been researched. Here in our study, we firstly identified circ-GALNT16 which could specifically interact with the KH3 domain of hnRNPK and enhance its SUMOylation modification via inhibiting SENP2 binding to hnRNPK. These results indicated that circRNA could regulate the SUMOylation modification of protein and opened a new insight for circRNA targeting therapy.

RNA-seq and following qRT-PCR verified that Serpine1 could be downregulated by circ-GALNT16 through the hnRNPK-p53 complex. Several studies have reported that Serpine1 is elevated in multiple tumor tissues and correlates with poor outcomes, including colorectal cancer. P53 and NF-κB both have been reported to participate in Serpine1 transcriptional regulation (43–45). But the particular mechanisms of Serpine1 remain unclear, especially in CRC. Besides, a previous study had reported that SUMOylation of hnRNPK generated different effects on individual p53 target gene through regulating the sequence-specific DNA binding ability of p53 (26). Therefore, after we found that the inhibition of hnRNPK deSUMOylation caused by circ-GALNT16 overexpression could inhibit Serpine1 expression, we proved that circ-GALNT16 overexpression could upregulate the p21 mRNA level through the hnRNPK-p53 complex, which was corresponding with the previous study (26). Intriguingly, ChIP assay showed that circ-GALNT16 could attenuate the enrichment of hnRNPK and p53 at Serpine1 promoters but facilitate the enrichment at p21 promoters. The underlying mechanisms deserved further investigation.

To explore how circ-GALNT16 mediated the SUMOylation of hnRNPK, we identified SENP2, which was reported to antagonistically mediate the hnRNPK SUMOylation in HeLa and HCC cells, could interact with hnRNPK in CRC cells (17, 26). Furthermore, overexpression of circ-GALNT16 could attenuate the interaction between hnRNPK and SENP2, while circ-GALNT16 knockdown enhanced their interaction. But we did not find out how circ-GALNT16 mediated the interaction between SENP2 and hnRNPK and the SUMOylation of hnRNPK through binding to the KH3 domain of hnRNPK specifically. However, a previous study had investigated that PSTAR could also inhibit the SENP2-mediated deSUMOylation of hnRNPK through interacting with the KH3 domain, which is consistent with our result (26). Hence, we believe there must be some kind of correlation between them.

In this study, we revealed the tumor suppression effect and feasible molecular mechanisms of the novel circRNA, circ-GALNT16, in colorectal cancer. The extreme downregulation of circ-GALNT16 in CRC tissues indicated that circ-GALNT16 might serve as a diagnostic and prognostic biomarker. Our mice model showed circ-GALNT16 overexpression could inhibit the proliferation and metastasis ability of CRC *in vivo*, which indicated that circ-GALNT16 might have the potential to act as a therapeutic target for CRC.

Conclusions

In summary, we identified a novel circRNA, named circ-GALNT16, that was downregulated in CRC and negatively associated with poor prognosis. Circ-GALNT16 could suppress the proliferation and aggressiveness of CRC cells and attenuate Serpine1 expression through inhibiting SENP2-mediated

hnRNPK deSUMOylation and adjusting the sequence-specific DNA binding ability of the hnRNPK-p53 complex.

Abbreviations

CRC: colorectal cancer; circRNA: circular RNA; GALNT16: polypeptide N-acetylgalactosaminyltransferase 16; hnRNPK: heterogeneous nuclear ribonucleoprotein K; SUMO1: small ubiquitin-related modifier 1; OS: overall survival rate; GAPDH: glyceraldehyde 3-phosphate dehydrogenase; SENP2: SUMO specific peptidase 2; Serpine1: serpin family E member 1; EDU: 5-Ethynyl-2'-deoxyuridine; CCK8: Cell Counting Kit-8; IHC: immunohistochemistry; qRT-PCR: quantitative reverse transcription polymerase chain reaction; FISH: Fluorescence in situ hybridization; MS: mass spectrometry; RBPs: RNA binding proteins; NEM: N-ethylmaleimide; shRNA: short hairpin RNA; HCC: hepatocellular carcinoma; FKBP4: FKBP prolyl isomerase 4; PI3K□phosphatidylinositol 3-kinase; AKT: AKT serine/threonine kinase 1.

Declarations

Ethics approval and consent to participate

This study was approved by the Ethics Committee of the First Affiliated Hospital with Nanjing Medical University.

Consent for publication

Not applicable.

Availability of data and materials

The data supporting the findings of this article is included within this article and its additional files.

Competing interests

The authors declare that they have no competing interests.

Funding

This study was supported by Jiangsu Provincial Natural Science Foundation for Basic Research, China (Grant No. BK20201491), the National Key R&D Program of China (2017YFC0908200), and Jiangsu Key Medical Discipline (General Surgery; Grant No. ZDxKA2016005).

Authors' contributions

Chaofan Peng, Wen Peng, Junwei Tang, and Yueming Sun generated the hypothesis and designed the study. Chaofan Peng, Yuqian Tan, Peng Yang performed experiments. Kangpeng Jin and Chuan Zhang performed the animal experiments. Chaofan Peng, Yifei Feng, Lu Wang, Jiahui Zhou, Ranran Chen,

Jiangzhou Ji, Tuo Wang, Chi Jin interpreted the data. Chaofan Peng wrote the manuscript. Yueming Sun and Junwei Tang supervised the overall research, secured funding, and interpreted results.

Acknowledgments

We would like to thank the Core Facility of Jiangsu Provincial People's Hospital for its help in the detection of experimental samples. The authors thank Andy Zhao for her kindly supports during this study.

Author details

[1]Department of General Surgery, The First Affiliated Hospital of Nanjing Medical University, Nanjing, China

[2]The First School of Clinical Medicine, Nanjing Medical University, Nanjing, China

[3]Nanjing Medical University, Nanjing, China.

References

1. Siegel RL, Miller KD, Goding Sauer A, Fedewa SA, Butterly LF, Anderson JC, et al. Colorectal cancer statistics, 2020. CA Cancer J Clin. 2020;70(3):145-64.
2. Siegel RL, Miller KD, Jemal A. Cancer statistics, 2020. CA Cancer J Clin. 2020;70(1):7-30.
3. Vo JN, Cieslik M, Zhang Y, Shukla S, Xiao L, Zhang Y, et al. The Landscape of Circular RNA in Cancer. Cell. 2019;176(4):869-81 e13.
4. Chen LL. The expanding regulatory mechanisms and cellular functions of circular RNAs. Nat Rev Mol Cell Biol. 2020;21(8):475-90.
5. Kristensen LS, Andersen MS, Stagsted LVW, Ebbesen KK, Hansen TB, Kjems J. The biogenesis, biology and characterization of circular RNAs. Nat Rev Genet. 2019;20(11):675-91.
6. Yang H, Li X, Meng Q, Sun H, Wu S, Hu W, et al. CircPTK2 (hsa_circ_0005273) as a novel therapeutic target for metastatic colorectal cancer. Mol Cancer. 2020;19(1):13.
7. Su M, Xiao Y, Ma J, Tang Y, Tian B, Zhang Y, et al. Circular RNAs in Cancer: emerging functions in hallmarks, stemness, resistance and roles as potential biomarkers. Mol Cancer. 2019;18(1):90.
8. Jian X, He H, Zhu J, Zhang Q, Zheng Z, Liang X, et al. Hsa_circ_001680 affects the proliferation and migration of CRC and mediates its chemoresistance by regulating BMI1 through miR-340. Mol Cancer. 2020;19(1):20.
9. Du WW, Yang W, Li X, Awan FM, Yang Z, Fang L, et al. A circular RNA circ-DNMT1 enhances breast cancer progression by activating autophagy. Oncogene. 2018;37(44):5829-42.
10. Liu Y, Ma C, Qin X, Yu H, Shen L, Jin H. Circular RNA circ_001350 regulates glioma cell proliferation, apoptosis, and metastatic properties by acting as a miRNA sponge. J Cell Biochem.

2019;120(9):15280-7.

11. Chen Z, Ren R, Wan D, Wang Y, Xue X, Jiang M, et al. Hsa_circ_101555 functions as a competing endogenous RNA of miR-597-5p to promote colorectal cancer progression. Oncogene. 2019;38(32):6017-34.
12. Zhao H, Chen S, Fu Q. Exosomes from CD133(+) cells carrying circ-ABCC1 mediate cell stemness and metastasis in colorectal cancer. J Cell Biochem. 2020;121(5-6):3286-97.
13. Zheng X, Chen L, Zhou Y, Wang Q, Zheng Z, Xu B, et al. A novel protein encoded by a circular RNA circPPP1R12A promotes tumor pathogenesis and metastasis of colon cancer via Hippo-YAP signaling. Mol Cancer. 2019;18(1):47.
14. Wang Z, Qiu H, He J, Liu L, Xue W, Fox A, et al. The emerging roles of hnRNPK. J Cell Physiol. 2020;235(3):1995-2008.
15. Xu Y, Wu W, Han Q, Wang Y, Li C, Zhang P, et al. Post-translational modification control of RNA-binding protein hnRNPK function. Open Biol. 2019;9(3):180239.
16. Ritchie SA, Pasha MK, Batten DJ, Sharma RK, Olson DJ, Ross AR, et al. Identification of the SRC pyrimidine-binding protein (SPy) as hnRNP K: implications in the regulation of SRC1A transcription. Nucleic Acids Res. 2003;31(5):1502-13.
17. Lee SW, Lee MH, Park JH, Kang SH, Yoo HM, Ka SH, et al. SUMOylation of hnRNP-K is required for p53-mediated cell-cycle arrest in response to DNA damage. EMBO J. 2012;31(23):4441-52.
18. Pelisch F, Pozzi B, Risso G, Munoz MJ, Srebrow A. DNA damage-induced heterogeneous nuclear ribonucleoprotein K sumoylation regulates p53 transcriptional activation. J Biol Chem. 2012;287(36):30789-99.
19. Moumen A, Masterson P, O'Connor MJ, Jackson SP. hnRNP K: an HDM2 target and transcriptional coactivator of p53 in response to DNA damage. Cell. 2005;123(6):1065-78.
20. Li J, Peng W, Yang P, Chen R, Gu Q, Qian W, et al. MicroRNA-1224-5p Inhibits Metastasis and Epithelial-Mesenchymal Transition in Colorectal Cancer by Targeting SP1-Mediated NF-kappaB Signaling Pathways. Front Oncol. 2020;10:294.
21. Ding L, Zhao Y, Dang S, Wang Y, Li X, Yu X, et al. Circular RNA circ-DONSON facilitates gastric cancer growth and invasion via NURF complex dependent activation of transcription factor SOX4. Mol Cancer. 2019;18(1):45.
22. Zhang Z, Li J, Huang Y, Peng W, Qian W, Gu J, et al. Upregulated miR-1258 regulates cell cycle and inhibits cell proliferation by directly targeting E2F8 in CRC. Cell Prolif. 2018;51(6):e12505.
23. Yang P, Li J, Peng C, Tan Y, Chen R, Peng W, et al. TCONS_00012883 promotes proliferation and metastasis via DDX3/YY1/MMP1/PI3K-AKT axis in colorectal cancer. Clin Transl Med. 2020;10(6):e211.
24. Ji L, Li X, Zhou Z, Zheng Z, Jin L, Jiang F. LINC01413/hnRNP-K/ZEB1 Axis Accelerates Cell Proliferation and EMT in Colorectal Cancer via Inducing YAP1/TAZ1 Translocation. Mol Ther Nucleic Acids. 2020;19:546-61.

25. Peng W, Zhang C, Peng J, Huang Y, Peng C, Tan Y, et al. Lnc-FAM84B-4 acts as an oncogenic lncRNA by interacting with protein hnRNPK to restrain MAPK phosphatases-DUSP1 expression. Cancer Lett. 2020;494:94-106.
26. Qin G, Tu X, Li H, Cao P, Chen X, Song J, et al. Long Noncoding RNA p53-Stabilizing and Activating RNA Promotes p53 Signaling by Inhibiting Heterogeneous Nuclear Ribonucleoprotein K deSUMOylation and Suppresses Hepatocellular Carcinoma. Hepatology. 2020;71(1):112-29.
27. Zhou WY, Cai ZR, Liu J, Wang DS, Ju HQ, Xu RH. Circular RNA: metabolism, functions and interactions with proteins. Mol Cancer. 2020;19(1):172.
28. Bomsztyk K, Denisenko O, Ostrowski J. hnRNP K: one protein multiple processes. Bioessays. 2004;26(6):629-38.
29. Ostrowski J. Transient recruitment of the hnRNP K protein to inducibly transcribed gene loci. Nucleic Acids Research. 2003;31(14):3954-62.
30. Expert-Bezancon A, Le Caer JP, Marie J. Heterogeneous nuclear ribonucleoprotein (hnRNP) K is a component of an intronic splicing enhancer complex that activates the splicing of the alternative exon 6A from chicken beta-tropomyosin pre-mRNA. J Biol Chem. 2002;277(19):16614-23.
31. Lubelsky Y, Ulitsky I. Sequences enriched in Alu repeats drive nuclear localization of long RNAs in human cells. Nature. 2018;555(7694):107-11.
32. Xu Y, Chen W, Liang J, Zeng X, Ji K, Zhou J, et al. The miR-1185-2-3p-GOLPH3L pathway promotes glucose metabolism in breast cancer by stabilizing p53-induced SERPINE1. J Exp Clin Cancer Res. 2021;40(1):47.
33. Wang Q, Lu W, Yin T, Lu L. Calycosin suppresses TGF-beta-induced epithelial-to-mesenchymal transition and migration by upregulating BATF2 to target PAI-1 via the Wnt and PI3K/Akt signaling pathways in colorectal cancer cells. J Exp Clin Cancer Res. 2019;38(1):240.
34. Wei X, Li S, He J, Du H, Liu Y, Yu W, et al. Tumor-secreted PAI-1 promotes breast cancer metastasis via the induction of adipocyte-derived collagen remodeling. Cell Commun Signal. 2019;17(1):58.
35. Xi X, Liu N, Wang Q, Chu Y, Yin Z, Ding Y, et al. ACT001, a novel PAI-1 inhibitor, exerts synergistic effects in combination with cisplatin by inhibiting PI3K/AKT pathway in glioma. Cell Death Dis. 2019;10(10):757.
36. Bi J, Liu H, Dong W, Xie W, He Q, Cai Z, et al. Circular RNA circ-ZKSCAN1 inhibits bladder cancer progression through miR-1178-3p/p21 axis and acts as a prognostic factor of recurrence. Mol Cancer. 2019;18(1):133.
37. Zhang C, Zhang C, Lin J, Wang H. Circular RNA Hsa_Circ_0091579 Serves as a Diagnostic and Prognostic Marker for Hepatocellular Carcinoma. Cell Physiol Biochem. 2018;51(1):290-300.
38. Guo G, Wang H, Ye L, Shi X, Yan K, Lin K, et al. Hsa_circ_0000479 as a Novel Diagnostic Biomarker of Systemic Lupus Erythematosus. Front Immunol. 2019;10:2281.
39. Yang F, Fang E, Mei H, Chen Y, Li H, Li D, et al. Cis-Acting circ-CTNNB1 Promotes beta-Catenin Signaling and Cancer Progression via DDX3-Mediated Transactivation of YY1. Cancer Res. 2019;79(3):557-71.

40. Chen LY, Wang L, Ren YX, Pang Z, Liu Y, Sun XD, et al. The circular RNA circ-ERBIN promotes growth and metastasis of colorectal cancer by miR-125a-5p and miR-138-5p/4EBP-1 mediated cap-independent HIF-1alpha translation. Mol Cancer. 2020;19(1):164.
41. Xue D, Wang H, Chen Y, Shen D, Lu J, Wang M, et al. Circ-AKT3 inhibits clear cell renal cell carcinoma metastasis via altering miR-296-3p/E-cadherin signals. Mol Cancer. 2019;18(1):151.
42. Wong CH, Lou UK, Li Y, Chan SL, Tong JH, To KF, et al. CircFOXK2 Promotes Growth and Metastasis of Pancreatic Ductal Adenocarcinoma by Complexing with RNA-Binding Proteins and Sponging MiR-942. Cancer Res. 2020;80(11):2138-49.
43. Zeng C, Chen Y. HTR1D, TIMP1, SERPINE1, MMP3 and CNR2 affect the survival of patients with colon adenocarcinoma. Oncol Lett. 2019;18(3):2448-54.
44. Li S, Wei X, He J, Tian X, Yuan S, Sun L. Plasminogen activator inhibitor-1 in cancer research. Biomed Pharmacother. 2018;105:83-94.
45. Szoltysek K, Janus P, Zajac G, Stokowy T, Walaszczyk A, Widlak W, et al. RRAD, IL4I1, CDKN1A, and SERPINE1 genes are potentially co-regulated by NF-kappaB and p53 transcription factors in cells exposed to high doses of ionizing radiation. BMC Genomics. 2018;19(1):813.

Figures

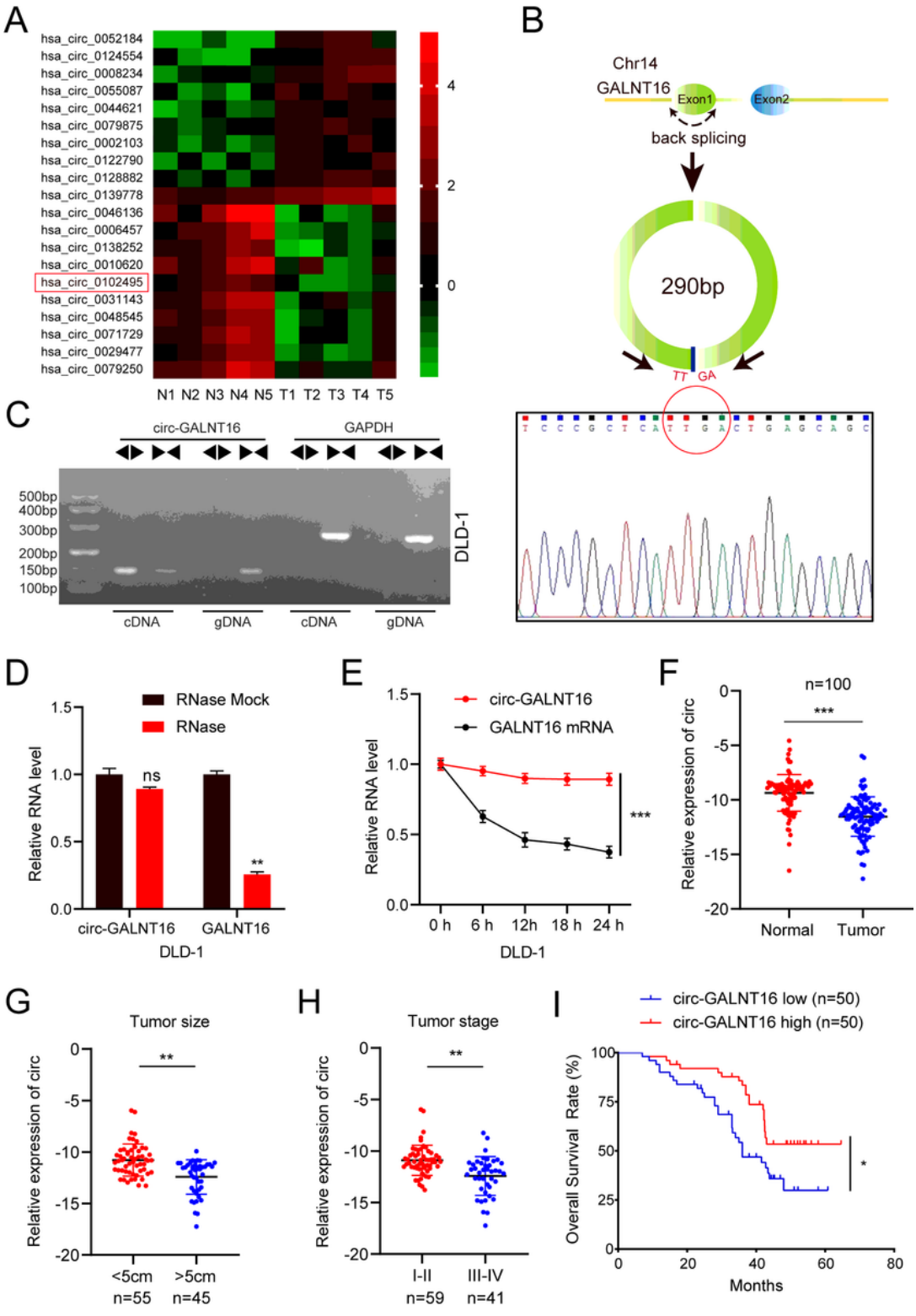

Figure 1

Circ-GALNT16 validation and expression in CRC cells and tissues. a. Heatmap of top ten upregulated and downregulated expression circRNAs between CRC tissues and adjacent normal tissues according to the circRNA microarray. b. The schematic illustration showed the back splicing of circ-GALNT16 and sanger sequence validated the splicing site. c. PCR and agarose gel electrophoresis confirmed the circular formation of circ-GALNT16, using divergent and convergent primers in gDNA and cDNA of DLD-1. GAPDH

was used as a negative control. d, e. Circ-GALNT16 and linear GALNT16 expression levels were detected after RNase R or actinomycin D treatment in DLD-1. f. Relative circ-GALNT16 expression in 100 CRC tissues and matched adjacent normal tissues. g-h. Relative expression of circ-GALNT16 in different tumor size and tumor stage groups. i. Kaplan-Meier plots of the overall survival of CRC patients with high (n =50) and low (n = 50) levels of circ-GALNT16. All data are presented as the means ± SD of three independent experiments. ns p >0.05, *p < 0.05, **p < 0.01, ***p < 0.001.

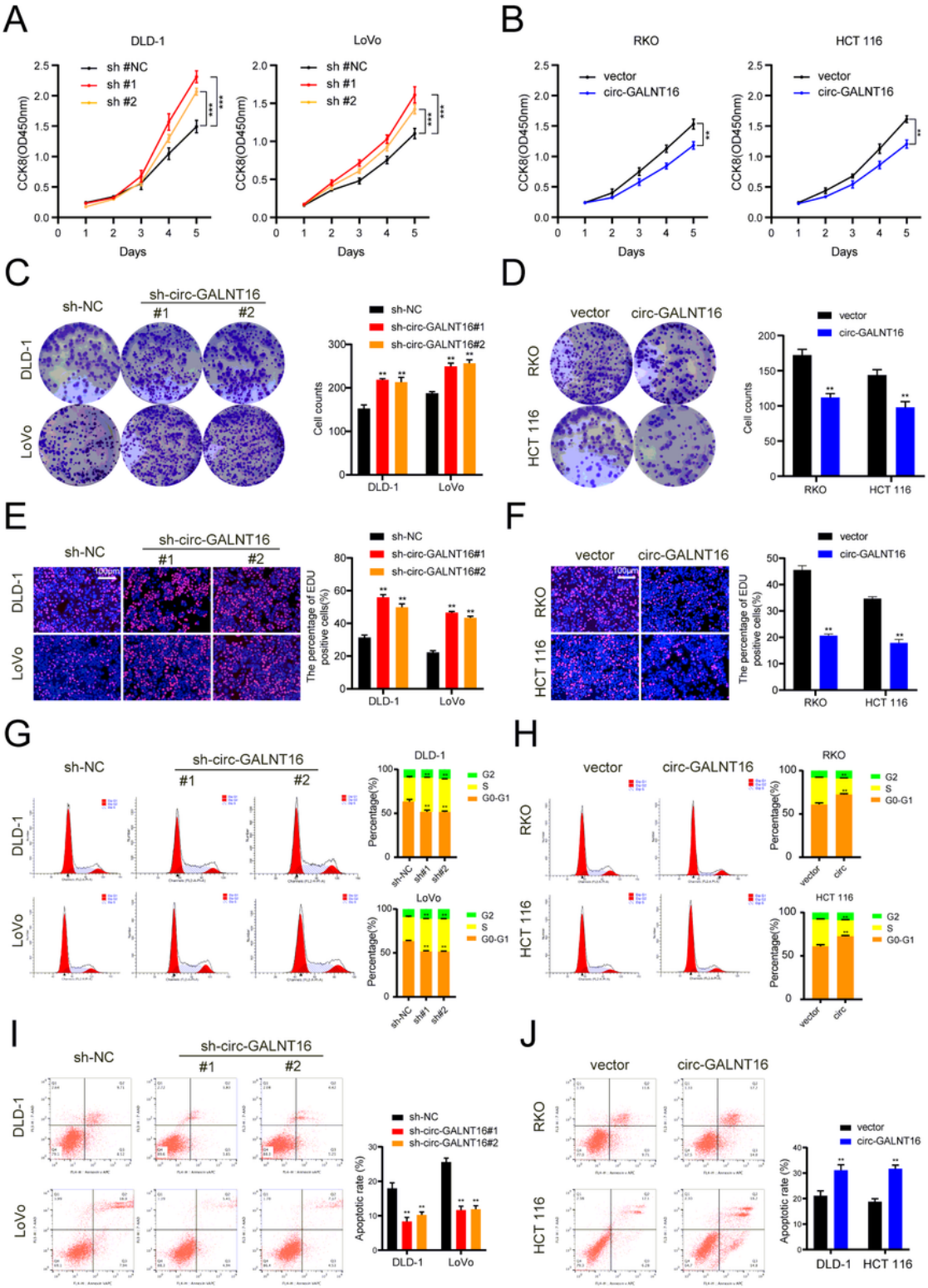

Figure 2

Circ-GALNT16 suppresses the proliferation of CRC cells in vitro. a, b. CCK8 assays were applied to determine the growth curves of circ-GALNT16 knockdown or overexpression cells. c, d. Colony formation assays were performed to evaluate cell proliferation ability. e, f. EdU assays were performed to assess the cell proliferation ability. g, h. Cell cycle distributions were detected by flow cytometry in circ-GALNT16 knockdown or overexpression cells. i, j. The apoptotic rates were performed and analyzed after treated with 0.5mM H202. All data are presented as the means ± SD of three independent experiments. **p < 0.01, ***p < 0.001.

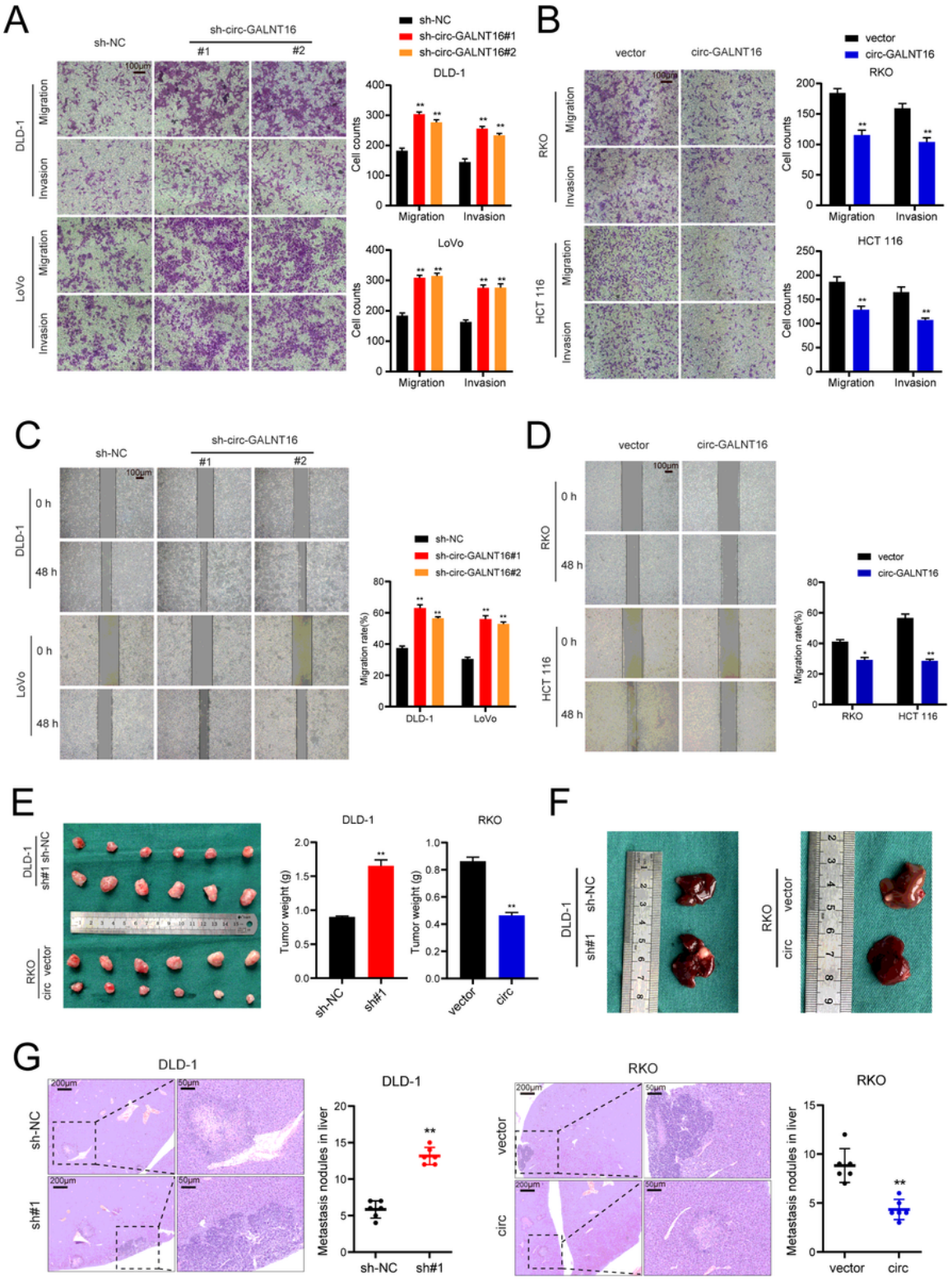

Figure 3

Effects of circ-GALNT16 on the proliferation, migration, and invasion in vitro and vivo. a, b. Transwell assays were applied to evaluate the migration and invasion abilities of CRC cells. c, d. Cell migration ability was assessed by wound healing assay. e. Representative photographs of subcutaneous xenograft tumors were obtained from nude mice, and the tumor weights were measured. f, g. Representative images and HE staining of liver metastatic tumors. All data are presented as the means ± SD of three independent experiments. *p < 0.05, **p < 0.01.

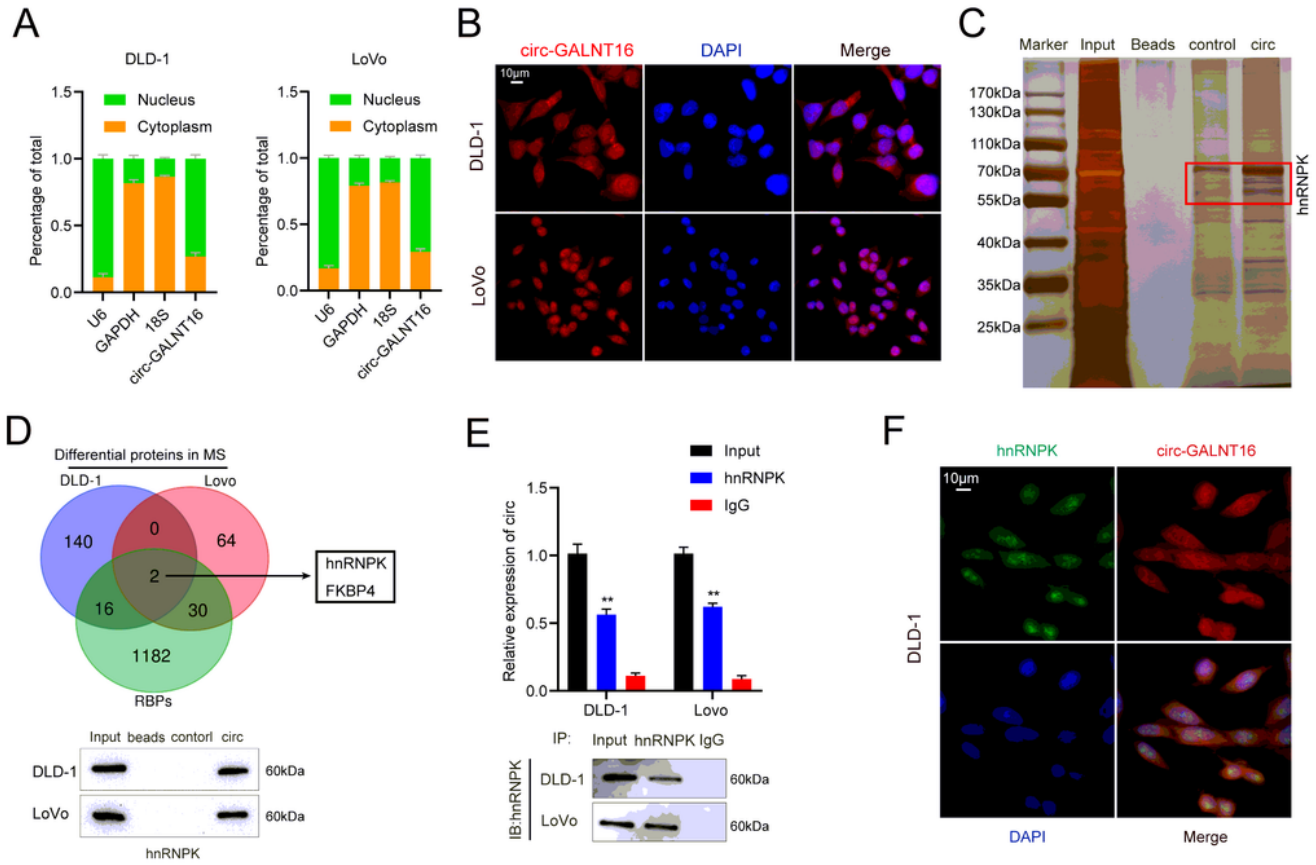

Figure 4

Circ-GALNT16 is mainly localized in the nucleus and binds to the KH3 domain of hnRNPK. a, b. Subcellular fractionation and FISH assays indicated that circ-GALNT16 was predominately localized in the nucleus of CRC cells. c-e. RNA pulldown assay followed by silver staining, MS, and RIP assay indicated that circ-GALNT16 specifically interacted with hnRNPK. f. Dual RNA FISH and immunofluorescence assays showed that circ-GALNT16 and hnRNPK colocalized in the nucleus of DLD-1. g. Functional domain and truncated mutation annotation of hnRNPK. h-i. RIP assay and RNA pulldown assay confirmed that circ-GALNT16 characteristically interacted with the KH3 domain of hnRNPK. j. The protein level of hnRNPK in circ-GALNT16 knockdown and overexpression cells. k. The circ-GALNT16 expression level in hnRNPK silencing cells.ns $p > 0.05$, $^{**}p < 0.01$.

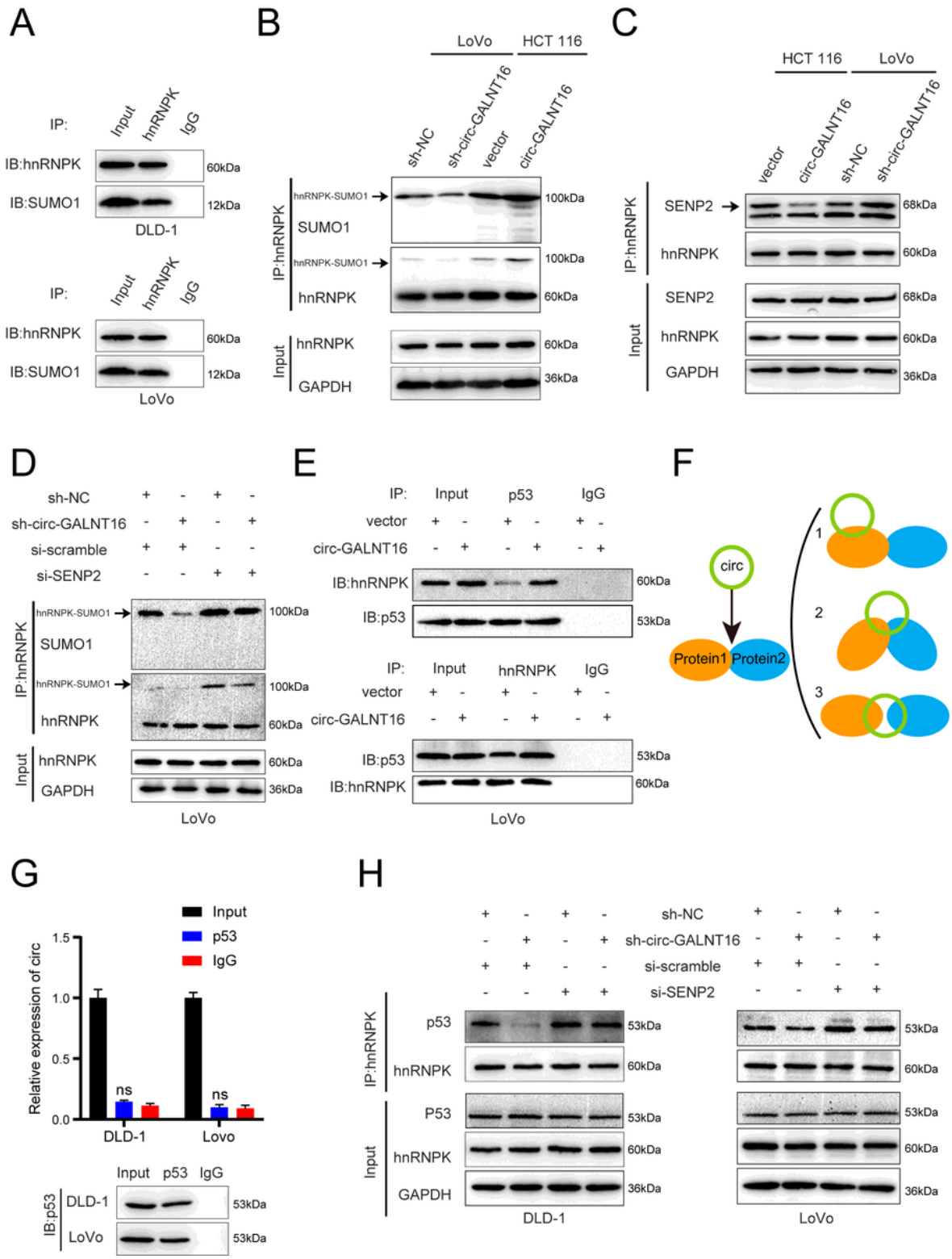

Figure 5

Circ-GALNT16 promotes the interaction between hnRNPK and p53 via inhibiting SENP2-mediated deSUMOylation. a. Co-IP assay was performed in protein lysate pulled down by circ-GALNT16 specifical probe using anti-hnRNPK. b. SUMOylation modification analysis was performed to identify the levels of hnRNPK SUMOylation in circ-GALNT16 knockdown and overexpression cells. c. The co-IP assay was performed between SENP2 and hnRNPK in circ-GALNT16 silencing and overexpression cells. d.

SUMOylation modification analysis to explore the levels of hnRNPK SUMOylation in circ-GALNT16 knockdown and SENP2 knockdown cells. e. The co-IP assay elucidated that circ-GALNT16 could mediate the interaction between hnRNPK and p53. f. Three modes of circRNA-protein interactions. g. RIP assay showed p53 did not interact with circ-GALNT16 directly. h. Co-IP assay between p53 and hnRNPK applied in circ-GALNT16 and SENP2 depletion cells. All data are presented as the means ± SD of three independent experiments. ns p >0.05, **p < 0.01.

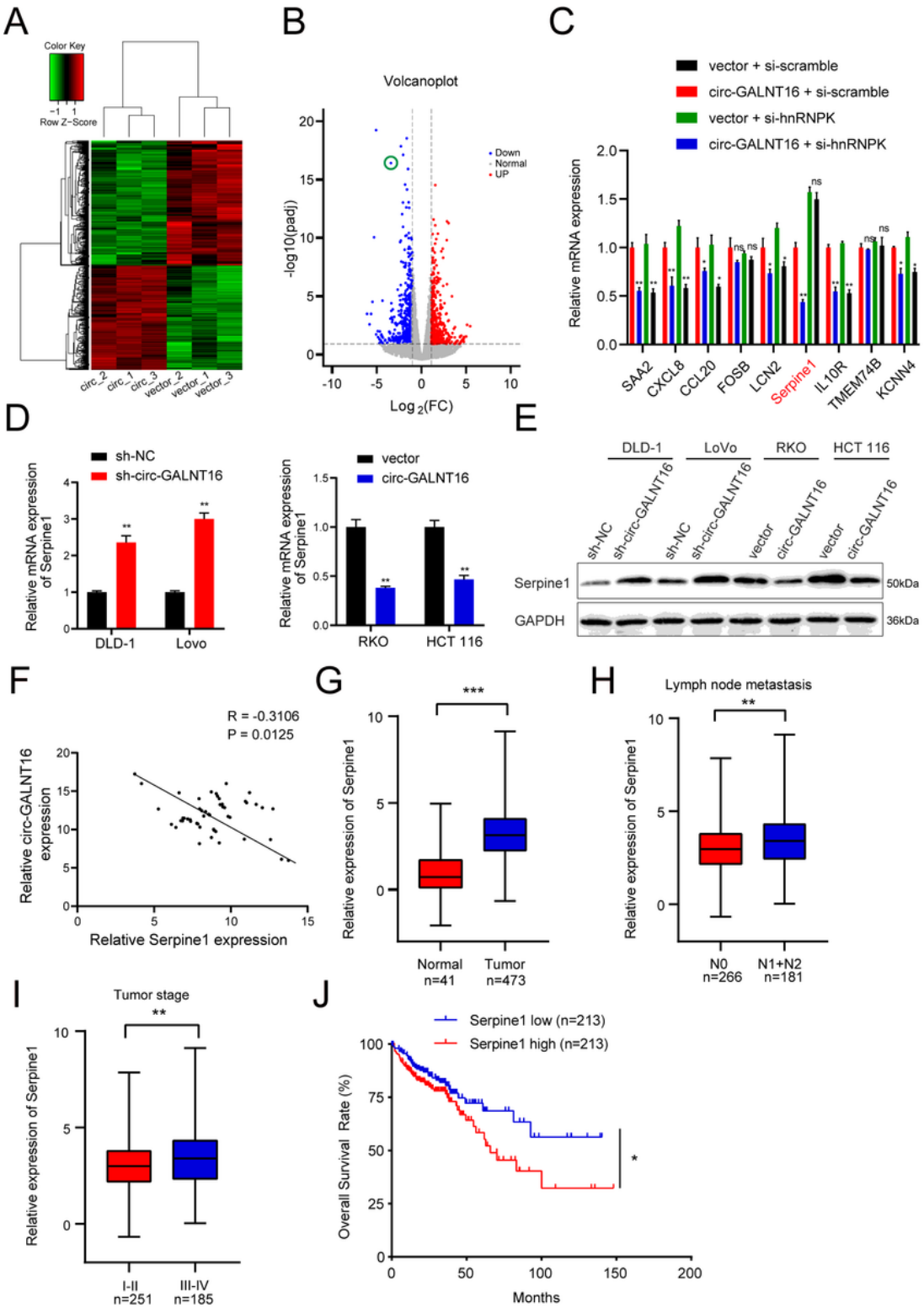

Figure 6

Serpine1 is downregulated by circ-GALNT16 and has a connection with CRC progression. a, b. Heatmap and scatter diagram showed the RNA-seq result in circ-GALNT16 overexpression and control RKO cells. c. Several candidates were validated by qRT-PCR. d, e. The mRNA and protein levels of Serpine1 in circ-GALNT16 knockdown and overexpression cells. f. Correlation analysis between circ-GALNT16 and Serpine1. (R = -0.3106, P = 0.0125) g-j. Serpine1 expression in CRC and the correlation with relative clinical features analysis from TCGA. All data are presented as the means ± SD of three independent experiments. ns p >0.05, *p < 0.05, **p < 0.01, ***p < 0.001.

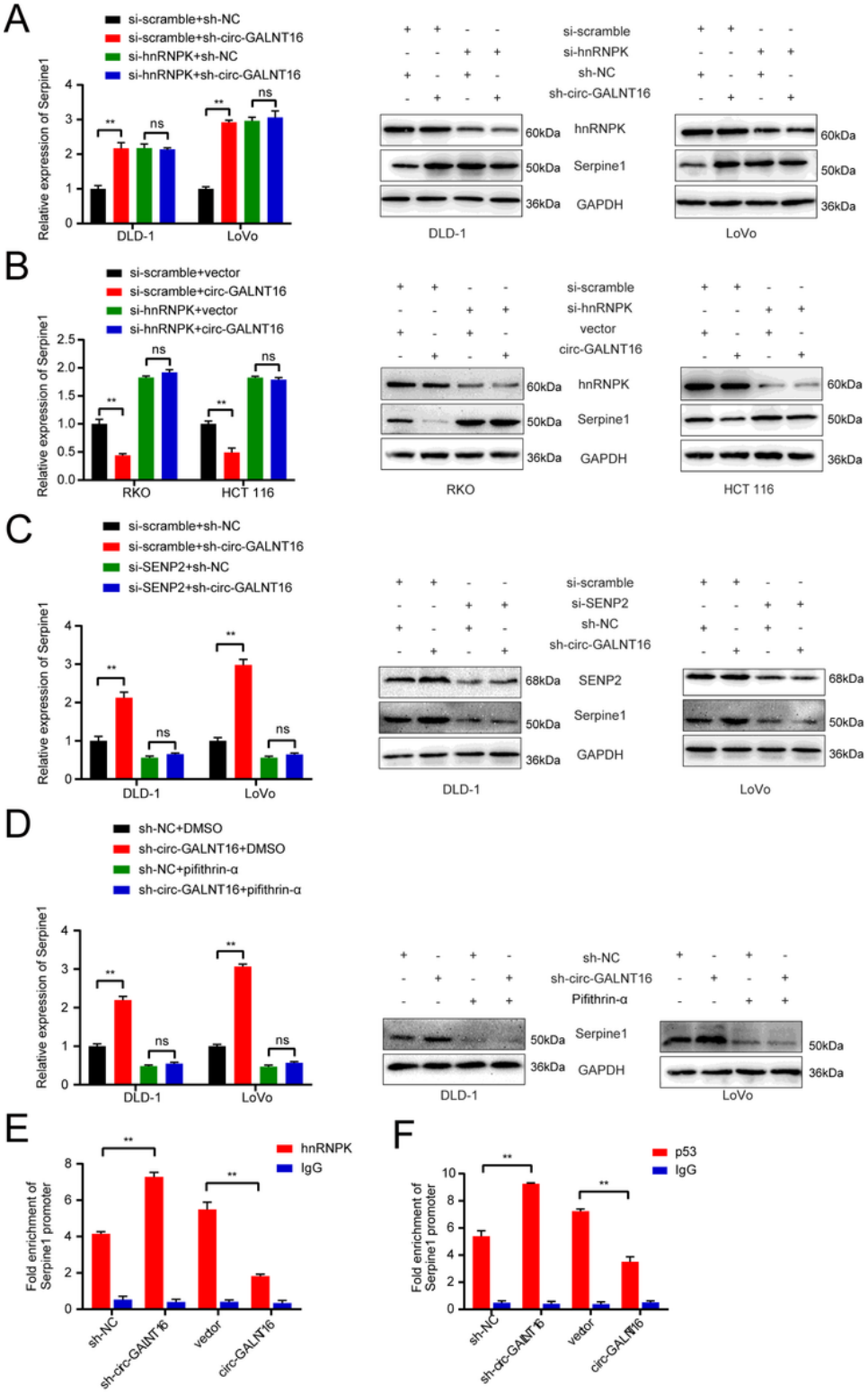

Figure 7

Circ-GALNT16 regulates Serpine1 through the SUMOylation of hnRNPK and p53. a, b. The mRNA and protein level of Serpine1 was detected in circ-GALNT16 knockdown and overexpression cells while hnRNPK was silenced. c. The expression of Serpine1 was detected in circ-GALNT16 knockdown cells while SENP2 was silenced. d. The expression of Serpine1 in circ-GALNT16 silencing cells was detected with the Pifithrin-α (10μM) treatment. e, f. HnRNPK and p53 chromatin immunoprecipitation were performed to measure the hnRNPK and p53 enrichment at the promoter region(s) of Serpine1. All data are presented as the means ± SD of three independent experiments. ns $p > 0.05$, **$p < 0.01$.

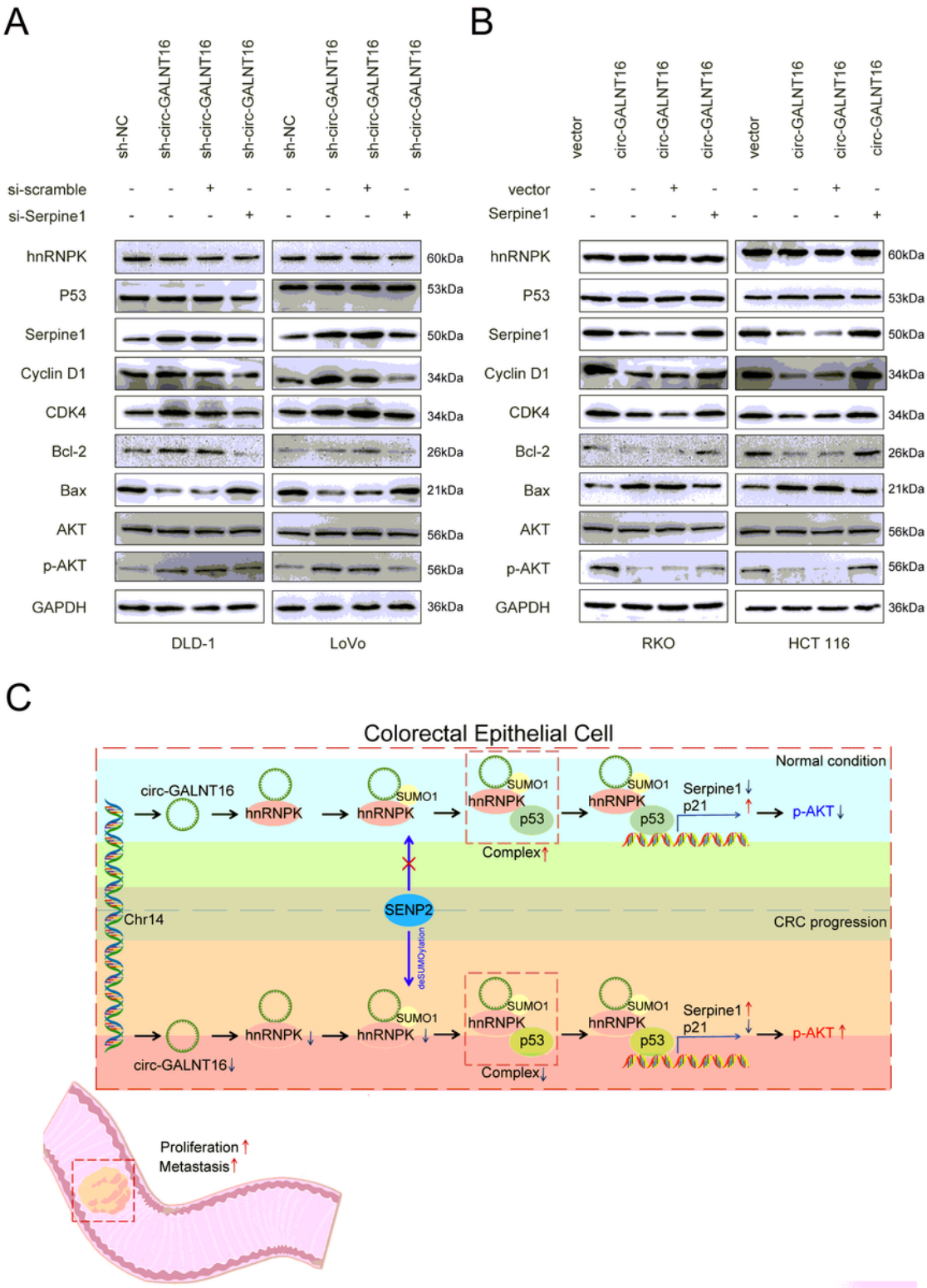

Figure 8

Circ-GALNT16 suppresses the CRC growth and metastasis through PI3K/AKT pathway. a, b. HnRNPK, p53, Serpine1, Cyclin D1, CDK4, Bcl-2, Bax, AKT, p-AKT expression were detected in relatively treated cells. c. A schematic model for the mechanisms of circ-GALNT16 in CRC.

Supplementary Files

This is a list of supplementary files associated with this preprint. Click to download.

- Additionalfile1Fig.S1.tif
- Additionalfile10TableS1.xlsx
- Additionalfile11Table.S2.xlsx
- Additionalfile12Table.S3.xlsx
- Additionalfile13Table.S4.docx
- Additionalfile14Table.S5.xlsx
- Additionalfile15Table.S6.xlsx
- Additionalfile2Fig.S2.tif
- Additionalfile3Fig.S3.tif
- Additionalfile4Fig.S4.tif
- Additionalfile5Fig.S5.tif
- Additionalfile6Fig.S6.tif
- Additionalfile7Fig.S7.tif
- Additionalfile8Fig.S8.tif
- Additionalfile9Fig.S9.tif
- Additionalfilesinformation.docx